THE JOURNAL OF BIOLOGICAL CHEMISTRY VOL. 287, NO. 50, pp. 41820–41834, December 7, 2012

Zeaxanthin Protects Plant Photosynthesis by Modulating Chlorophyll Triplet Yield in Specific Light-harvesting Antenna Subunits*[S]

Received for publication, July 28, 2012, and in revised form, October 12, 2012 Published, JBC Papers in Press, October 12, 2012, DOI 10.1074/jbc.M112.405498

Luca Dall'Osto[‡], Nancy E. Holt[‡§], Shanti Kaligotla[¶], Marcel Fuciman[¶], Stefano Cazzaniga[‡], Donatella Carbonera[‖], Harry A. Frank[¶], Jean Alric[§], and Roberto Bassi[‡§‡‡1]**

*From the [‡]Dipartimento di Biotecnologie, Università di Verona, Strada Le Grazie 15, 37134 Verona, Italy, [§]Laboratoire de Genetique et Biophysique des Plantes, Faculté des Sciences de Luminy Case 901 136 Avenue de Luminy, 13288 Marseille Cedex 9, France, the [¶]Department of Chemistry, University of Connecticut, Storrs, Connecticut 06269, [‖]Dipartimento di Scienze Chimiche, Università di Padova, Via Marzolo 1, 35131 Padova, Italy, **Unité Mixte de Recherche 7141 CNRS-Université Paris 6, Institut de Biologie Physico-Chimique, 13 rue Pierre et Marie Curie, 75005 Paris, France, and [‡‡]Phytosphäre Forschungszentrum Jülich, 52425 Jülich, Germany*

Background: The plant carotenoid zeaxanthin is accumulated under excess light.
Results: Zeaxanthin induces a red shift in the carotenoid triplet excited state spectrum and reveals a higher efficiency in controlling chlorophyll triplet formation.
Conclusion: Binding of zeaxanthin to specific proteins modulates the yield of dangerous chlorophyll excited states and protects photosynthesis from over-excitation.
Significance: Functional dissection of zeaxanthin-dependent photoprotective mechanisms is crucial for understanding how plants avoid photoinhibition.

Plants are particularly prone to photo-oxidative damage caused by excess light. Photoprotection is essential for photosynthesis to proceed in oxygenic environments either by scavenging harmful reactive intermediates or preventing their accumulation to avoid photoinhibition. Carotenoids play a key role in protecting photosynthesis from the toxic effect of over-excitation; under excess light conditions, plants accumulate a specific carotenoid, zeaxanthin, that was shown to increase photoprotection. In this work we genetically dissected different components of zeaxanthin-dependent photoprotection. By using time-resolved differential spectroscopy *in vivo*, we identified a zeaxanthin-dependent optical signal characterized by a red shift in the carotenoid peak of the triplet-minus-singlet spectrum of leaves and pigment-binding proteins. By fractionating thylakoids into their component pigment binding complexes, the signal was found to originate from the monomeric Lhcb4–6 antenna components of Photosystem II and the Lhca1–4 subunits of Photosystem I. By analyzing mutants based on their sensitivity to excess light, the red-shifted triplet-minus-singlet signal was tightly correlated with photoprotection in the chloroplasts, suggesting the signal implies an increased efficiency of zeaxanthin in controlling chlorophyll triplet formation. Fluorescence-detected magnetic resonance analysis showed a decrease in the amplitude of signals assigned to chlorophyll triplets belonging to the monomeric antenna complexes of Photosystem II upon zeaxanthin binding; however, the amplitude of carotenoid triplet signal does not increase correspondingly. Results show that the high light-induced binding of zeaxanthin to specific proteins plays a major role in enhancing photoprotection by modulating the yield of potentially dangerous chlorophyll-excited states *in vivo* and preventing the production of singlet oxygen.

Plants are particularly prone to photo-oxidative damage for the same reasons that they are effective at photosynthesis, namely because the primary pigment chlorophyll (Chl)[2] is a very efficient sensitizer. The singlet excited states of Chl molecules (^{1}Chl*) are efficiently quenched by photochemical reaction centers. Nevertheless, environmental conditions easily unbalance the ratio between energy capture and utilization; *e.g.* at high photon flux densities, accumulation of excitons in the light-harvesting complexes (Lhc) of both photosystems (PS) increases the amount of ^{1}Chl*. This raises the probability of intersystem crossing to the Chl triplet state (^{3}Chl*), a species that reacts with molecular oxygen (O_2) to yield singlet oxygen ($^1O_2$) molecules (1). Because of the high reactivity and low diffusion radius of $^1O_2$, this reactive oxygen species (ROS) induces damage in its local environment by (2), destroying lipids and nucleic acids and proteins (3–5), thus leading to a loop of ever-

* This work was supported by grants from the Marie Curie Actions - Networks for Initial Training Harvest (Grant no. PITN-GA-2009-238017) and PRIN Programmi di Ricerca di Interesse Nazionale (Grant no. 2008XB774B) (to R. B.). Work in the laboratory of H. A. F. was supported by grants from the National Science Foundation (MCB-0913022) and the UConn Research Foundation.
[S] This article contains supplemental Tables S1–S3 and Fig. S1–S6.
The nucleotide sequence(s) reported in this paper has been submitted to the GenBank™/EBI Data Bank with accession number(s) At5G57030, At1G08550, At5G67030, and At1G44446.
[1] To whom correspondence should be addressed: University of Verona, Biotechnology Department, Strada Le Grazie 15, 37134 Verona, Italy. Tel.: 39-045-8027916; Fax: 39-045-8027929; E-mail: roberto.bassi@univr.it.

[2] The abbreviations used are: Chl, chlorophyll; Lhc, light-harvesting complex; PS, photosystem; ROS, reactive oxygen species; Car, carotenoid; Zea, zeaxanthin; EL, excess light; Vio, violaxanthin; qE, excitation quenching; TmS, triplet-minus-singlet; FDMR, fluorescence-detected magnetic resonance; EL, excess light; α-DM, α-dodecylmaltoside; SOSG, singlet oxygen sensor green; RT, room temperature; NPQ, non-photochemical quenching; qZ, Zea-dependent component of NPQ.

increasing $^1O_2$ production and further oxidation until photobleaching (6). This photooxidative damage leads to a dramatic depression of photosynthetic efficiency called photoinhibition (7–9).

A second pigment class essential for photosynthesis is represented by carotenoids (Car), whose photoprotective action in the photosynthetic apparatus is well established (10). Carotenoids are either carotenes, bound to PSI and PSII core complexes, or their oxygenated derivatives, xanthophylls, mainly bound to Lhc proteins. Xanthophylls are involved in a number of photoprotection mechanisms, being active in (i) preventing over-excitation of reaction centers by quenching ^{1}Chl* states (11), (ii) quenching ^{3}Chl* through carotenoid triplet (^{3}Car*) formation, thus avoiding ROS formation (12), and (iii) scavenging ROS (13). Among xanthophylls, zeaxanthin (Zea) is of particular interest because it is absent in dark or low light conditions and only accumulates in excess light (EL), where it is produced from the diepoxide xanthophyll violaxanthin (Vio) (14) through the action of the violaxanthin de-epoxidase enzyme (15, 16). Zea is known to be involved in several types of photoprotection events of the PSII reaction center, which occur on varying timescales. A number of these mechanisms quench ^{1}Chl*, namely (i) feedback de-excitation quenching (qE) (17, 18), which occurs on the timescale of seconds to minutes, (ii) a slowly inducible quenching or qZ (19), which is likely caused by Zea binding to Lhc upon exchange with Vio (20), and (iii) a long term, irreversible quenching that reflects a photoinhibitory state of PSII (21). An increase of thermal dissipation of ^{1}Chl* can effectively protect reaction centers from over-excitation, thus reducing the probability of intersystem crossing to ^{3}Chl* and $^1O_2$ formation in the Lhcs.

Previous results (22) demonstrated that the *npq1* mutant of *Arabidopsis thaliana*, which is defective in the light-dependent Vio to Zea interconversion, shows increased photoinhibition and lipid peroxidation with respect to wild type (WT) in EL, leading to a decreased fitness (23). Early suggestions pointed to the decreased capacity for quenching of singlet excited chlorophylls (qE) (11). Further work by comparing the *npq1* to the *npq4* mutant, the latter lacking qE but retaining the ability for Zea synthesis, showed that protection of thylakoid membrane lipids against photooxidation was provided by a mechanism different than ^{1}Chl* quenching (22). Moreover, besides its role in singlet energy dissipation, Zea has been proposed to act as an antioxidant by scavenging $^1O_2$ and thus preventing lipid peroxidation (24) upon its release from the pH-dependent V1 binding site of the major LHCII complex (25, 26) into the lipid phase. However, a fundamental understanding of the Zea-dependent photoprotection mechanism, its location and whether its significance in providing overall photoprotection *in vivo* is mainly dependent on either ^{1}Chl*/^{3}Chl* quenching or ROS scavenging remains and awaits a more detailed analysis of the contributions of the different mechanisms involved in photoresistance.

Once synthesized, Zea has a dual location; it can be either free into thylakoid membrane lipids or bound to the Lhc proteins (27, 28). The effect of the former pool was investigated in *Arabidopsis* showing that Zea has a distinct capacity for scavenging ROS with respect to other xanthophyll species (29). Furthermore, it has been reported (30, 31) that the photoprotective effect of xanthophylls is greatly enhanced by their binding to Lhc proteins. Therefore, besides ROS scavenging in the lipid phase (32) and enhancing of qE (11), a third photoprotective effect is provided by a mechanism specifically exerted by the Lhc-bound Zea pool.

Here, we show that Zea bound to specific Lhcs is directly involved in the modulation of ^{3}Chl*. By means of time-resolved spectroscopy *in vivo*, we found that the photoresistance of *Arabidopsis* to EL treatment tightly correlates with the detection of a red shift in the major carotenoid signal in triplet-minus-singlet (TmS) spectra upon Zea synthesis, as measured in intact leaves. Fractionation of thylakoid membranes from EL-treated plants allowed detection of the red-shifted TmS signal in the monomeric Lhcb subunits of PSII (Lhcb4–6) and the dimeric Lhca subunits of PSI but not in the major trimeric LHCII complex. In each case the Zea-dependent red shift correlates with a reduced yield of $^1O_2$ production from purified Lhc proteins or from photosynthetic supercomplexes containing these subunits. Analysis by fluorescence-detected magnetic resonance (FDMR) at 4 K showed decreased amplitude of ^{3}Chl* upon Zea binding, implying a Zea-specific effect in decreasing the yield of dangerous excited states. We conclude that, in addition to the previously described effects in quenching ^{1}Chl* and scavenging $^1O_2$, an additional photoprotection mechanism is elicited by Zea binding to specific Lhc protein subunits consisting of a reduction in the yield in harmful ^{3}Chl*.

EXPERIMENTAL PROCEDURES

Plant Material

WT plants of *A. thaliana* and mutants *lut2* (lacking lutein (Lut)), *npq1* (unable to synthesize zeaxanthin in high light), *npq2* (retaining lutein and zeaxanthin as only xanthophylls), and *ch1* (lacking chlorophyll *b*) were obtained from NASC (ecotype Col-0). Mutants *npq1lut2*, *npq2lut2*, *ch1npq1*, *ch1lut2* were isolated by crossing single mutant plants. Plants were grown for 4 weeks on Sondermisch potting mix (Gramoflor) in controlled conditions (~120 μmol of photons m^{-2} s^{-1}, 23 °C, 8 h light/16 h dark) before measurements.

Thylakoid Isolation and Sample Preparation

Stacked thylakoid membranes were isolated from either dark-adapted or excess light (EL)-treated leaves (33). Grana membranes have been isolated from dark- and EL-treated samples using α-dodecylmaltoside (α-DM) solubilization of stacked thylakoids, as described in Ref. 34. Membranes corresponding to 500 μg of chlorophylls were washed with 5 mM EDTA, solubilized with 0.6% α-DM, and then fractionated by ultracentrifugation in a 0.1–1 M sucrose gradient as previously described (25). Purified monomeric Lhcb proteins (band 2 in the sucrose gradient) were further fractionated by flat-bed isoelectric focusing at 4 °C (35). Purified LHCI complexes were obtained as described in Ref. 36.

Pigment Analysis

Pigments were extracted either from whole leaves, thylakoid membranes, or isolated antenna complexes with 80% acetone then separated and quantified by HPLC (37).

Determination of the Sensitivity to Photooxidative Stress

Short term EL treatment was performed for 1 h at 1200 μmol photons m^{-2} s^{-1} at RT (22 °C) to obtain the maximum Zea accumulation on detached leaves floating on water. Light was provided by 150 watt halogen lamps (Focus3, Prisma, Italy). Samples for HPLC analysis were rapidly frozen in liquid nitrogen before pigment extraction. EL-treated leaves used for thylakoid isolation were vacuum-infiltrated with 50 μM Norfluorazon (a zeaxanthin-epoxidase inhibitor) upon EL treatment to slow down Zea-Vio conversion (38) during thylakoid isolation procedure. Photo-destruction of pigment-protein complexes *in vivo* was induced by a strong light treatment; leaf discs floating on water were exposed to high light (2500 μmol of photon m^{-2} s^{-1}) at RT for 31 h. For the quantification of Lhcb subunits, frozen leaf discs were homogenized in liquid nitrogen, and protein was extracted in 62.5 mM Tris-HCl, pH 6.8, 10% glycerol, 2% SDS, 5% β-mercaptoethanol. For each sample, the same volume of leaf extract (corresponding to 0.5 μg of chlorophylls of t_0 sample) was loaded on SDS-PAGE. Immunoblot assays with antibodies against different polypeptides were performed as described previously (39). To avoid any deviation between different immunoblots, samples were compared only when loaded in the same slab gel.

Spectroscopy

Steady State Spectroscopy—Spectra were obtained using samples in 10 mM Hepes, pH 7.5, 0.06% α-DM, 0.2 M sucrose. Absorption measurements were performed using a SLM-Aminco DW-2000 spectrophotometer at RT.

Time-resolved Spectroscopy—absorbance changes were monitored in purified proteins or intact *Arabidopsis* leaves with a home-built pump and probe laser spectrophotometer basically described in Ref. 40) or with a laser flash photolysis spectrometer for isolated pigments. Transient absorption spectra were recorded in the laboratory of H. A. Frank at room temperature using an Edinburgh Instruments Model LP920KS flash photolysis spectrometer consisting of a Xe 920 450-watt arc lamp as a probe light source. The excitation pulse was generated by a Continuum Nd:YAG-pumped optical parametric oscillator laser tuned to excite selectively the Chl *a* Q_y band at 662 nm. The pump laser and probe light beams were configured perpendicular to each other. A Tektronix digital oscilloscope model TDS 3012B was used for signal averaging. All transient absorption profiles were the average of 20 scans. The solutions contained micromolar concentrations of Chl *a* (as a triplet donor), and the xanthophylls (as triplet acceptors) and were degassed using at least five freeze-pump-thaw cycles before the spectroscopic measurements.

Quantification of Singlet Oxygen Yield—Measurements of $^1O_2$ production on leaves and purified pigment-protein complexes were performed using Singlet Oxygen Sensor Green (SOSG, Invitrogen). SOSG is a fluorescent probe highly selective for $^1O_2$ that increase its 530-nm emission band in presence of this ROS; it was shown to be a useful and reliable probe for the detection of $^1O_2$ *in vivo* and in purified Lhcs (30, 41–43). Leaves were vacuum-infiltrated with the dye solution (SOSG 200 μM) and illuminated with red light ($\lambda > 600$ nm, 1200 or 400 μmol m^{-2} s^{-1}) at RT. The increase of SOSG-specific fluorescence emission was followed to quantify ROS release into leaves (λ_{exc} 480 nm, λ_{emis} 530 nm). Fluorescence emission spectra were measured at RT using a Jobin-Yvon Fluoromax-3 spectrofluorimeter equipped with a fiber optic to measure emission of fluorogenic probes on leaves. For the measurements of $^1O_2$ yield on either Lhc, PSII supercomplex, and PSI-LHCI, pigment-protein complexes were harvested from sucrose gradient and diluted in a reaction buffer (10 mM Hepes, pH 7.5, 0.06% α-DM, 2 μM SOSG) to the same absorption area in the wavelength range 600–750 nm (about 2.2 μg of Chls/ml). Isolated complexes were illuminated with red light ($\lambda > 600$ nm), and fluorescence yield of SOSG were determined before and during EL treatment to quantify $^1O_2$-dependent fluorescence increase (30). Upon EL treatment, we did not observe photobleaching of either chlorophyll or carotenoid in leaves or purified pigment-protein complexes.

FDMR—For all the experiments, the samples were dissolved in buffer to a concentration of 200 μg Chl/ml. Degassed glycerol was added (60% v/v) just before freezing the samples by direct immersion in liquid helium into the pre-cooled cryostat. FDMR experiments were performed in the laboratory-built apparatus, previously described in detail (44–46). In the specific experiments, the modulation frequency and the microwave power were chosen depending on the triplet state. The temperature of all the experiments performed was 1.8 K. All the FDMR spectra are presented as $\Delta I/I$, where ΔI is the fluorescence change induced by the resonant microwave field, and I is the steady state fluorescence detected by the photodiode. Because in all the experiments I remains substantially unmodified upon light treatments, the change of the intensity of $\Delta I/I$ signal after EL is a measure of the change in triplet yield.

Statistics

Significance analysis was performed using either Student's *t* test or analysis of covariance in GraphPad Prism (see the figure legends for details). *Error bars* represent the standard deviation.

Sequence data from this article can be found in the EMBL/GenBank™ data libraries under the following accession numbers: *lut2* (line N656231 with insertion into the lycopene-ϵ-cyclase gene, At5G57030); *npq1* (line N624757 with insertion into the violaxanthin-deepoxidase gene, At1G08550); *npq2* (line N559469 with insertion into the zeaxanthin-epoxidase gene, At5G67030); *ch1* (line N524295 with insertion into the chlorophyll-a oxygenase gene, At1G44446).

RESULTS

Effect of Zea-Lhc Interaction in Limiting $^1O_2$ Release from Arabidopsis Leaves under EL—When photosynthetic organisms are exposed to EL, photo-oxidative stress occurs with the production of $^1O_2$. Among the xanthophylls, Zea has been proposed to be the most active into scavenging of $^1O_2$ and preventing lipid peroxidation (29). To investigate the function of the Lhc-bound zeaxanthin pool, we analyzed the photoprotective efficacy of *A. thaliana* mutants that were deficient in their ability to synthesize Zea (*npq1*) either in a WT or *ch1* genetic background. The *ch1* mutation inactivates Chl *a* oxidase (47) and thus Chl *b* synthesis; see supplemental Table S1 for pigment

composition of these genotypes. Because Chl *b* is an essential co-factor for the assembly of Lhc pigment-protein complexes (48), a de-stabilization of Lhc proteins is obtained; the *ch1* mutation leads to a strong reduction of PS antenna size (49), whereas xanthophylls bound to Lhc in the WT are released into the membrane (29).

We evaluated $^1O_2$ release on leaf discs using SOSG (41), a $^1O_2$ highly selective fluorescence probe. After illumination of discs with EL (1200 μmol photons m^{-2} s^{-1}, RT), *ch1* leaves showed a far higher release of $^1O_2$ with respect to WT at each time point (supplemental Fig. S1) despite a 4-fold lower PSII antenna size (29). This observation is consistent with recent reports showing that the enhanced lipid peroxidation in *ch1* is due to $^1O_2$ attack on lipids (50) and that higher $^1O_2$ yield in *ch1* is attributed to the lack of xanthophyll binding complexes (30). To evaluate the photoprotection capacity of zeaxanthin in WT *versus ch1* background, intensity of EL was chosen for *npq1* and *ch1npq1* leaf discs to obtain the same $^1O_2$ yield; thus, WT and *npq1* discs were illuminated with 1200 μmol of photons m^{-2} s^{-1}, and *ch1* genotypes were illuminated with 400 μmol of photons m^{-2} s^{-1}. Results are reported in Fig. 1. The WT leaves exhibited a lower $^1O_2$ yield per chlorophyll relative to the *npq1* in EL (Fig. 1*A*), thus confirming the enhanced photoprotection capacity of Zea with respect to the other xanthophylls (29). However, Zea-dependent photoprotection is lower in *ch1* plants; clearly, the effect of the *npq1* mutation in increasing $^1O_2$ release was significant only in non-*ch1* genotypes (Fig. 1). These findings with *ch1* plants imply that, although Zea has a high photoprotective effect, its performance is strongly enhanced through binding to the Lhc proteins.

Measurements of Light-induced $^1O_2$ Yield on Purified Pigment-Protein Complexes—The results reported above suggest a role for Zea-Lhc interactions in the photoprotection of thylakoid membranes by preventing $^1O_2$ release into the lipid phase. Previous investigation on recombinant Lhcs (20) and *in vivo* (51) showed that Zea can bind to specific sites of Lhc subunits; in particular, xanthophyll exchange occurs in the inner L2 site of the minor antennae of Lhcb4 (CP29), Lhcb5 (CP26), Lhcb6 (CP24), and LHCI (51–53), whereas trimeric LHCII binds Zea to the external site V1 (25).

The differential level of $^1O_2$ production with *versus* without Zea is the signature of the Zea-dependent photoprotection mechanism and can be used for tracking the pigment-protein complexes responsible for this effect. To this aim, we compared the capacity for photoprotection of Lhcbs binding Vio or Zea by analyzing the amount of $^1O_2$ released by pigment-protein complexes isolated from either dark-adapted (Vio) or EL-treated (Zea) leaves. The $^1O_2$ yield was measured upon illumination of the complexes in the presence of SOSG. The pigment composition of purified complexes was analyzed by HPLC (supplemental Table S2). Binding of Zea to monomeric Lhcbs (a preparation of monomeric PSII antenna proteins that contains Lhcb4, Lhcb5, and Lhcb6 along with a fraction of monomerized LHCII complex) and LHCI (PSI antennae) significantly reduces the amount of $^1O_2$ produced in EL. Fig. 2, *A* and *C*, show that $^1O_2$ yield by monomeric Lhcb-Zea is reduced by 65% with respect to the Lhcb-Vio sample, the reduction being even greater in purified Lhcb5; likewise, the reduction in $^1O_2$ yield of

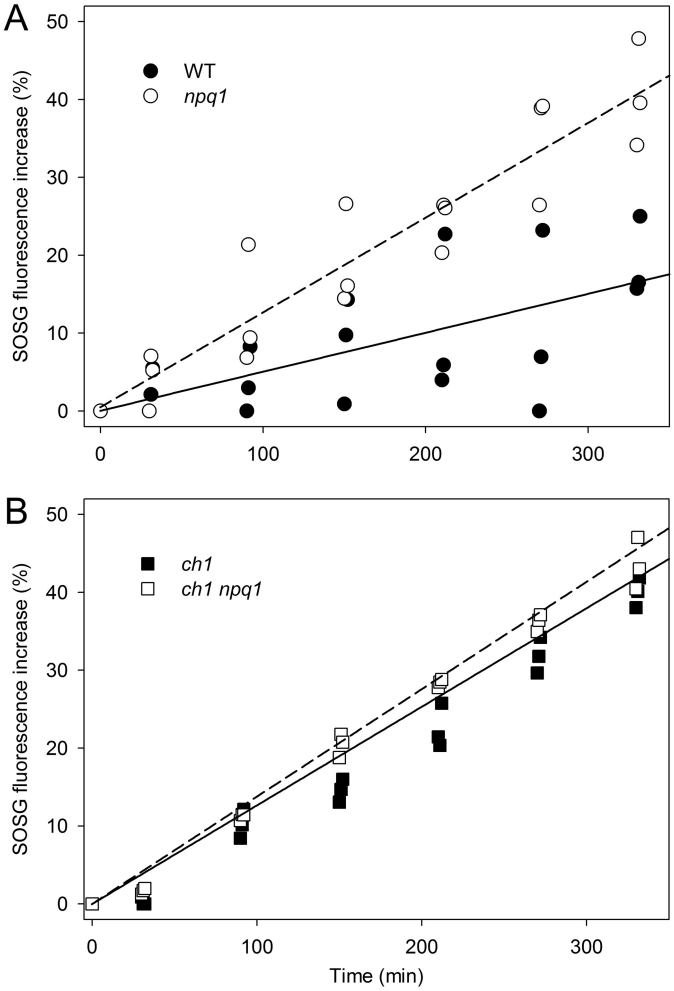

FIGURE 1. **Photoprotective role of Zea-Lhc interaction.** Singlet oxygen production from WT and xanthophyll mutants lacking Zea (*npq1*, *panel A*) and/or Lhc complexes (*ch1*, *panel B*) was measured on intact leaves upon illumination ($600 < \lambda < 750$ nm, RT, 1200 μmol of photons m^{-2} s^{-1} for WT and *npq1*, 400 μmol of photons m^{-2} s^{-1} for *ch1* background). The highly selective fluorescent probe SOSG was used to quantify light-dependent $^1O_2$ release, as its 530-nm emission band increases in proportion to the amount of this ROS released by the photosynthetic apparatus. Each experimental point corresponds to a different sample; these data are representative of two independent experiments. Experimental points were modeled with a linear regression. Statistical analysis (analysis of covariance) revealed that *npq1* leaves showed significantly higher $^1O_2$ production than wild type ($p = 0.0013$, *panel A*); instead, Zea-dependent photoprotection is less evident in *ch1* plants (differences between the slopes of *panel B* are not significant, $p = 0.55$).

LHCI-Zea *versus* LHCI-Vio is 40% at 700 μmol photons m^{-2} s^{-1} (Fig. 2*D*). These results imply that the Zea-containing complexes have a stronger capacity for photoprotection with respect to the same complexes binding Vio. Such an effect was not observed in trimeric LHCII, *i.e.* there was no change in $^1O_2$ yield based on its Vio or Zea content (Fig. 2*B*). When the production of $^1O_2$ was measured on both PSII supercomplexes (C_2S_2, see Ref. 54) and PSI-LHCI, complexes isolated from dark-adapted leaves (Vio binding) exhibited a 2-fold higher $^1O_2$ yield with respect to complexes isolated from EL-treated leaves (Zea binding) (Fig. 2, *E* and *F*, respectively). These results show that the lack of bound Zea to Lhc complexes negatively affects the photoprotective efficiency of the whole photosystem for both PSI and PSII.

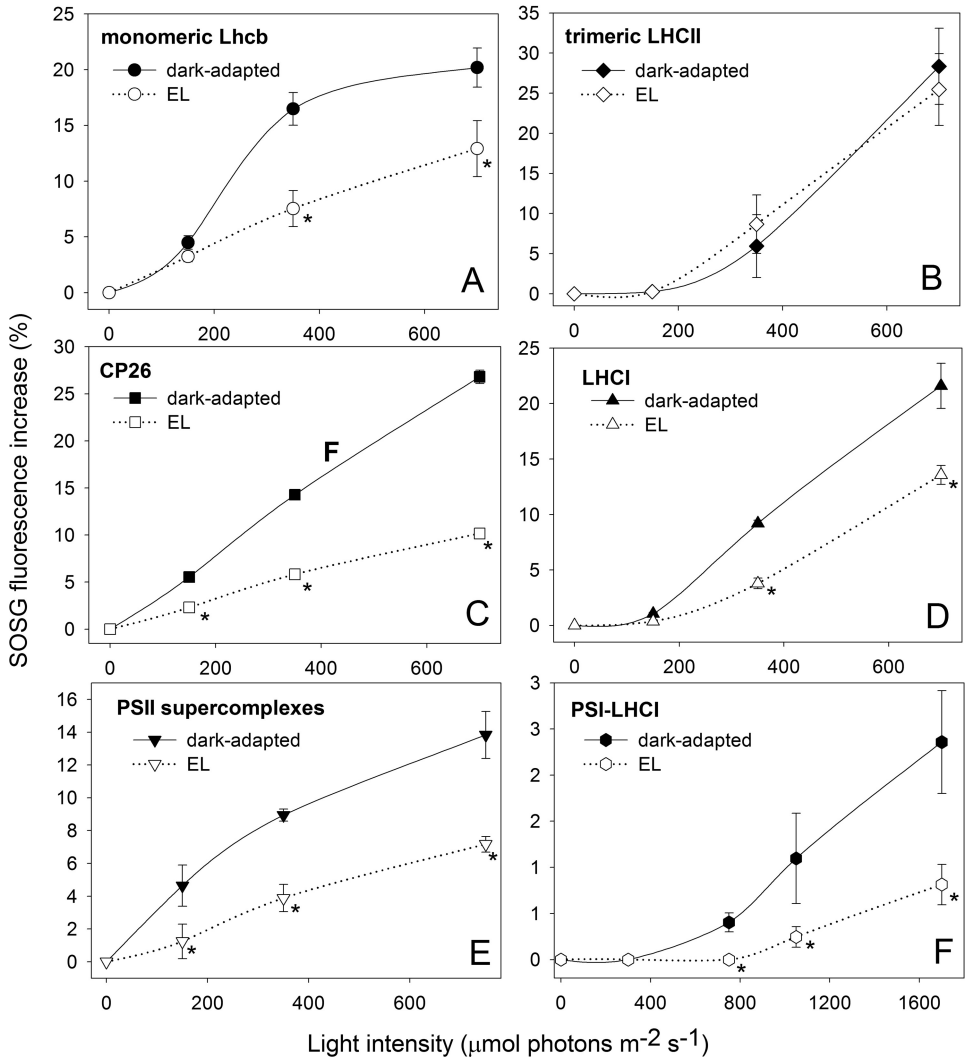

FIGURE 2. **Light-dependent singlet oxygen production from isolated pigment-proteins complexes.** SOSG was used to follow light-dependent $^1O_2$ release of pigment-protein complexes isolated from either dark-adapted or EL-treated leaves. Fluorescence of SOSG has been measured upon illumination of a solution containing monomeric Lhcb (*A*), trimeric LHCII (*B*), CP26 (*C*), and LHCI (*D*) with either Vio bound (*solid line*, *closed symbols*) or Zea bound (*dashed line*, *open symbols*) at different light intensities, 10 min each intensity. Trimeric LHCII isolated from either dark-adapted or EL-treated plants did not show significant differences in $^1O_2$ yield at all light intensities tested (*B*). Instead, Zea binding monomeric Lhcb, CP26, and LHCI showed significantly lower $^1O_2$ release than the Vio-binding complexes. Zea bound to these specific proteins plays a role in enhancing photoprotection by preventing the release of $^1O_2$ from either PSII (*E*) and PSI-LHCI (*F*) supercomplexes. *, $p < 0.05$ by Student's *t* test of Zea binding complexes relative to the corresponding Vio binding.

Among Lhcs, the components of the monomeric Lhcb fraction showed the highest reduction in $^1O_2$ yield upon binding Zea. To distinguish between the contributions of individual Lhc gene products, monomeric antennae fractions isolated from either dark-adapted and EL-treated WT leaves were further fractionated by preparative isoelectrofocusing; this purification procedure was shown to be affective in removing loosely bound pigments, such as xanthophyll bound to the external V1 site of LHCII, whereas xanthophylls of inner binding sites were retained (25). The pigment composition of purified complexes were analyzed by HPLC (supplemental Table S2); fraction 1 contained only monomeric LHCII and had a low content of Zea, whereas the fractions containing minor antennae had higher levels of Vio-Zea exchange. The fractions were further analyzed for their $^1O_2$ release upon EL treatment. Results are reported in Fig. 3; monomeric LHCII-Zea (fraction 1) did not show significant differences in $^1O_2$ yield with respect to LHCII-Vio (Fig. 3*A*); instead, fractions enriched in monomeric antennae (fractions 2–4) showed clear differences, with complexes from dark-adapted leaves yielding from 25% (CP29) to 65% (CP24) more $^1O_2$ with respect to the same complexes isolated from EL-treated leaves (Fig. 3, *B–D*).

Role of Zea-Lhc Interaction in the Photoprotection of PSII Antenna Subunits—The hypothesis that the lack of Zea might prevent activation of photoprotective mechanisms localized within monomeric Lhcs, thus enhancing ROS production specifically at the level of monomeric Lhcbs, was further investigated by analyzing WT and *npq1* genotypes for their capacity to resist degradation of Lhcb complexes *in vivo* upon exposure to EL. The kinetics of Lhcb photodegradation under strong light was quantified on total leaf extracts by immunoblotting with specific antibodies directed against different polypeptides supplemental Fig. S2). We observed that upon EL treatment the abundance in individual Lhcb polypeptides underwent a decay with rates that are affected by the presence/absence of Zea. A pronounced effect was clearly observed in the decay of minor

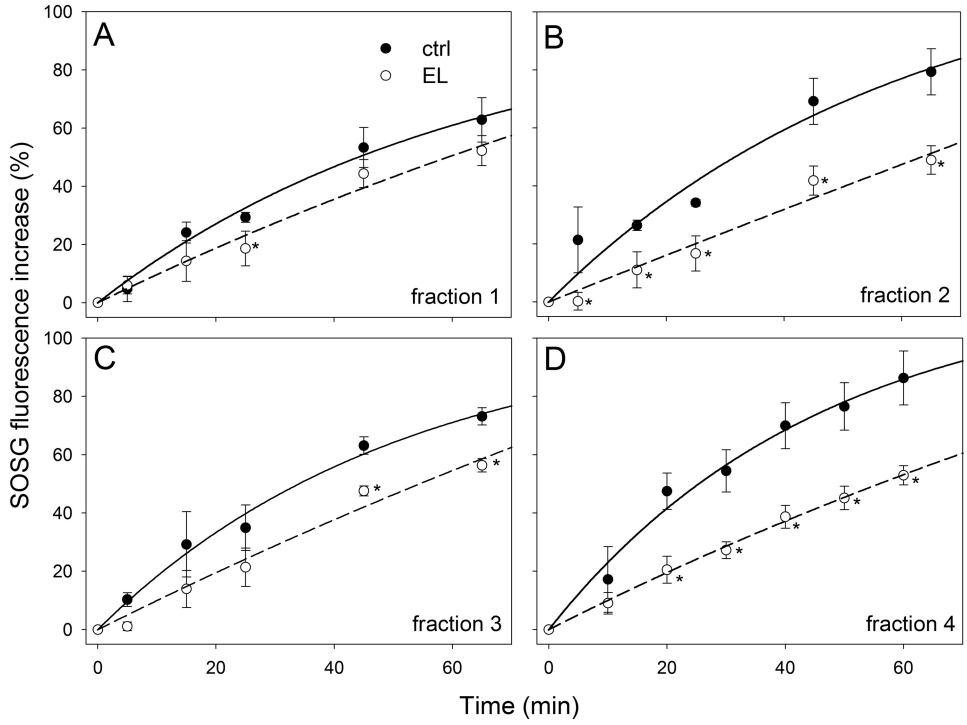

FIGURE 3. **Light-dependent $^1O_2$ release from monomeric Lhcb complexes.** SOSG was used to quantify light-dependent $^1O_2$ yield of monomeric Lhcb isolated by isoelectric focusing. Fluorescence of SOSG has been measured upon illumination of fractions containing monomeric LHCII (*A*) or enriched in minor antennae CP24 (*B*), CP29 (*C*), or CP26 (*D*) with either Vio bound (*closed symbols*) or Zea bound (*open symbols*) at 1000 μmol of photons m^{-2} s^{-1}. Monomeric LHCII isolated from either dark-adapted or EL-treated plants did not show any changes in $^1O_2$ yield (*A*). Zea binding monomeric Lhcbs (*B*, *C*, and *D*) showed significantly lower $^1O_2$ production than the Vio binding complexes. Thus, Zea bound to minor antennae plays a role in enhancing photoprotection by preventing the production of $^1O_2$. *, $p < 0.05$ by Student's *t* test of Zea binding complexes relative to the corresponding Vio binding.

antennae that depended on the WT or *npq1* genetic background, whereas the decay rate of the major LHCII polypeptides was only marginally affected if at all (supplemental Fig. S2). The decay for Lhcb4–6 degradation was clearly faster in *npq1* leaves (no Zea) than WT (+Zea) during EL stress, whereas no difference was observed in the case of LHCII (supplemental Fig. S2). We conclude that the Zea-dependent enhancement of photoprotection is located in monomeric Lhcs rather than in the major trimeric LHCII complex.

Time-resolved Laser Spectroscopy Measurements of the Car Triplet-excited States—Previous work has shown that ^{3}Chl* quenching and $^1O_2$ scavenging by xanthophylls ligands are the major determinants for the level of $^1O_2$ release by Lhc proteins upon EL treatment *in vitro* and *in vivo* (55, 56). To identify the physical mechanism(s) underlying the Zea-dependent photoprotective effect in plants, we measured the light-induced formation of triplet states (TmS spectra) upon excitation of Chl at 650 nm. These spectra are denoted TmS because they show the intersystem crossing of a pigment from its singlet state to its triplet state. The disappearance of the singlet state (S_0) and the appearance of the triplet state (T_1) are observed as a bleaching of the singlet absorbance bands ($S_2 \leftarrow S_0$) and the appearance of triplet absorbance bands ($T_2 \leftarrow T_1$). Such measurements of light-induced absorbance changes were done on a reconstituted *in vitro* suspension containing a mixture of Chl *a* and purified xanthophylls and *in vivo* on intact leaves from *Arabidopsis* genotypes differing in their capacity to synthesize Zea in EL (see supplemental Fig. S3, which compares the *in vivo* spectra with the triplet state spectra of Vio and Zea in solution, and supplemental Table S1 for pigment composition of the different genotypes). As expected, the kinetics and spectral response of the *in vitro* and *in vivo* systems were different because of the different environments (solvent or protein, respectively) surrounding the pigments. As commonly reported, the absorption peaks of pigments in solution are shifted toward shorter wavelengths as compared with what they are in the proteins, and due to diffusion, energy transfer between pigments in solution is slower than in their native environment. The data obtained on isolated pigments show that Zea is the "red-most carotenoid" (Table 1). It suggests that the substitution of Vio into Zea must translate into a red shift of the *in vivo* triplet spectrum of carotenoids.

On intact leaves a strong absorbance increase is instantly (<100 ns) observed at 520 nm after a flash of 650 ± 10-nm light (supplemental Fig. S3). The decay of this signal is biexponential, with half-times of ~2 μs and ~200 ms. Measurements of the dependence of each component on the intensity of the excitation light and the corresponding spectra at approximately maximum amplitude are shown in supplemental Fig. S3, C and D, respectively. The fast (~2 μs) component dominantly results from ^{3}Car*, whereas the slow component (~200 ms) is due to the electrochromic band-shift of carotenoids induced by transmembrane charge separation (57). Therefore, the TmS spectra of carotenoids can be deconvoluted from the electrochromic shift of carotenoids on the basis of their very different lifetimes. The amplitude of the triplet signal largely exceeds the amplitude of the bandshift signal, itself largely exceeding the $P700^+$ signal; indeed, in the spectral region 500–560 nm (Fig. 4) $P700^+$

TABLE 1

Singlet state, ϵ_S, and triplet state, ϵ_T, extinction coefficients of xanthophylls.

Extinction coefficients are at the wavelengths indicated in parentheses. The values are in units of L/mol·cm. The ϵ_S values were obtained from Britton *et al.* (80). The ϵ_T values were obtained as described in the text. ("Experimental Procedures - Spectroscopy")

Xanthophyll	ϵ_S	ϵ_T
	liters/mol·cm	*liters/mol·cm*
Violaxanthin	1.5×10^5 (440 nm)	4.2×10^5 (481 nm)
Zeaxanthin	1.4×10^5 (450 nm)	3.6×10^5 (510 nm)
Lutein	1.4×10^5 (445 nm)	3.2×10^5 (490 nm)
Neoxanthin	1.3×10^5 (440 nm)	3.6×10^5 (485 nm)

signal is very flat and of small amplitude (58). In the subsequent text, the fast microsecond component is referred as TmS (triplet-minus singlet) difference spectrum.

The TmS transition of WT, *npq1*, and *lut2* leaves, dark-adapted and after exposure to strong actinic light (to trigger the synthesis of Zea), in the 500–560-nm range that includes the ^{3}Car* transition are shown in Fig. 4. In comparing dark-adapted *versus* EL-treated leaves, a loss of signal was observed upon illumination in WT (Fig. 4*A*) and *lut2* (Fig. 4*C*) leaves between 500 and 520 nm (minimum at 505 nm), whereas a gain of signal was observed above 520 nm, with a maximum between 530 and 535 nm. Such an EL-induced red shift in ^{3}Car* transition level is expected from the de-epoxidation of Vio into Zea and from the red-most spectral contribution of the latter (supplemental Fig. S3). Consistently, the *npq1* mutation (Fig. 4*B*) abolished the red shift. It is worth noting that the amplitude of the ^{3}Car* red shift measured on intact leaves was proportional to the amount of Zea accumulated during EL treatment, which was not existent in *npq1*, greatest in *lut2*, and in-between the changes observed in *npq1* and *lut2* for WT leaves. These results show that Zea synthesis correlated with the formation of the red-shifted ^{3}Car* spectral form on intact leaves.

The red-shifted spectral form is likely to arise via ^{3}Chl* quenching rather than scavenging of $^1O_2$ because, although scavenging of $^1O_2$ by Zea occurs in the lipid phase (22, 29), it is very unlikely that it would be detected on timescales as short as 100 ns. To test this hypothesis, *ch1* mutants were investigated, as *ch1* plants lack Lhcb and have eight times more lipid-free xanthophylls than WT plants (30), implying that the red-shifted ^{3}Car* spectral form should be more evident in these mutants if it results from scavenging. Upon light-induced Zea synthesis, the *ch1lut2* plants (lacking both Lhcbs and Lut) did not undergo changes in the carotenoid TmS spectrum (Fig. 4*D*), although they do synthesize twice as much Zea than *lut2* plants (29). It seems plausible that β-carotene is the only carotenoid contributing to the TmS spectra of *ch1lut2* leaves; indeed in this genotype all xanthophylls are released into the thylakoid membrane, and β-carotene is the only carotenoid bound to chlorophyll-protein complexes, thus in condition to perform direct quenching of ^{3}Chl*. This is consistent with TmS spectrum reported for *ch1lut2* dark-adapted leaves, which showed a maximum even redder than that of EL-treated WT leaves; indeed, similar ^{3}Car* transition maxima have been reported for Zea and β-carotene (59). Additional measurements on mutants with different abilities for synthesizing Zea under EL treatment, namely *npq1lut2* and *npq2lut2*, showed that the formation of the red-shifted ^{3}Car* signal was associated with the extent of Vio to Zea conversion (Fig. 4, *E* and *F*). Moreover, TmS red shift still holds in a mutant lacking qE (*npq4lut2*, see supplemental Fig. S4) implying it is independent from PsbS, the protein essential for qE. Therefore, we conclude that the Car red shift observed is only due to Zea bound to the Lhc proteins serving as Chl *a*/*b*-xanthophyll binding antennas of photosystems.

Identification of Photosynthetic Subunits Involved in the Red Shift of Carotenoid Triplet Signal—To find the binding site for the Zea responsible for the red shift observed in the ^{3}Car* spectrum of leaves, we performed TmS spectroscopy measurements on proteins isolated from WT leaves that were either dark-adapted or treated with EL (Fig. 5; see supplemental Table S2 for pigment composition of purified complexes). Changes were observed in the monomeric Lhcb subunits (Fig. 5*A*) and LHCI (Fig. 5*D*)-containing fractions, whereas trimeric LHCII did not show any changes in the ^{3}Car* spectrum when isolated from EL-treated plants (Fig. 5*B*). These results suggest that both PSII and PSI have a specific Lhc target for Zea binding. A further fractionation of monomeric Lhcbs into antenna components revealed that changes in the ^{3}Car* spectrum were measured in all minor antennae (CP29, CP26, and CP24). Given by way of example, Fig. 5*C* compares TmS spectra from samples of CP26 containing either Vio or Zea (CP26 dark-adapted and CP26 EL, respectively) at the same Chl concentration. The peak amplitude of the CP26 dark-adapted sample is reduced by 45% with respect to CP26 EL, whereas the amount of absorption at wavelengths longer than 520 nm is ~60% higher in the CP26 EL sample containing Zea. In the LHCI samples containing either Vio or Zea (LHCI dark-adapted and LHCI EL, respectively) the peak was observed at 515 and 525 nm, respectively (Fig. 5*D*). We conclude that the TmS spectral shift observed *in vivo* tightly correlates with that detected in the LHCI and Lhcb4–6 subunits but not in the major trimeric LHCII complex. Moreover, both of these spectral features are associated with the major component of Zea-dependent photoprotection.

Investigation on the Chlorophyll-to-carotenoid Triplet Transfer—The mechanism(s) underlying the decreased production of $^1O_2$ upon Zea binding could be either (i) an increased efficiency in ^{3}Chl* quenching by xanthophylls bound to Lhc proteins or (ii) a direct down-regulation of the chlorophyll triplet yield, as compared with other de-excitation pathways. To distinguish between these two hypotheses, we assessed both the total amount of ^{3}Car* and the kinetics of ^{3}Car* formation in isolated pigment-protein complexes by time-resolved TmS spectroscopy. For this experiment, we chose the monomeric CP26 protein purified from dark-adapted or EL-treated WT leaves; in the latter, both (i) the Zea-dependent reduction of $^1O_2$ release (Fig. 2*C*) and (ii) the red shift in TmS spectra (Fig. 5*C*) were observed.

For an estimation of ^{3}Car* formed upon chlorophyll excitation, the TmS spectra of CP26 was fitted with ^{3}Car* spectral forms in a protein environment (Fig. 6), obtained by measuring recombinant LHC reconstituted with single xanthophyll species.[3] Although this deconvolution problem might have more

[3] R. Bassi, unpublished results.

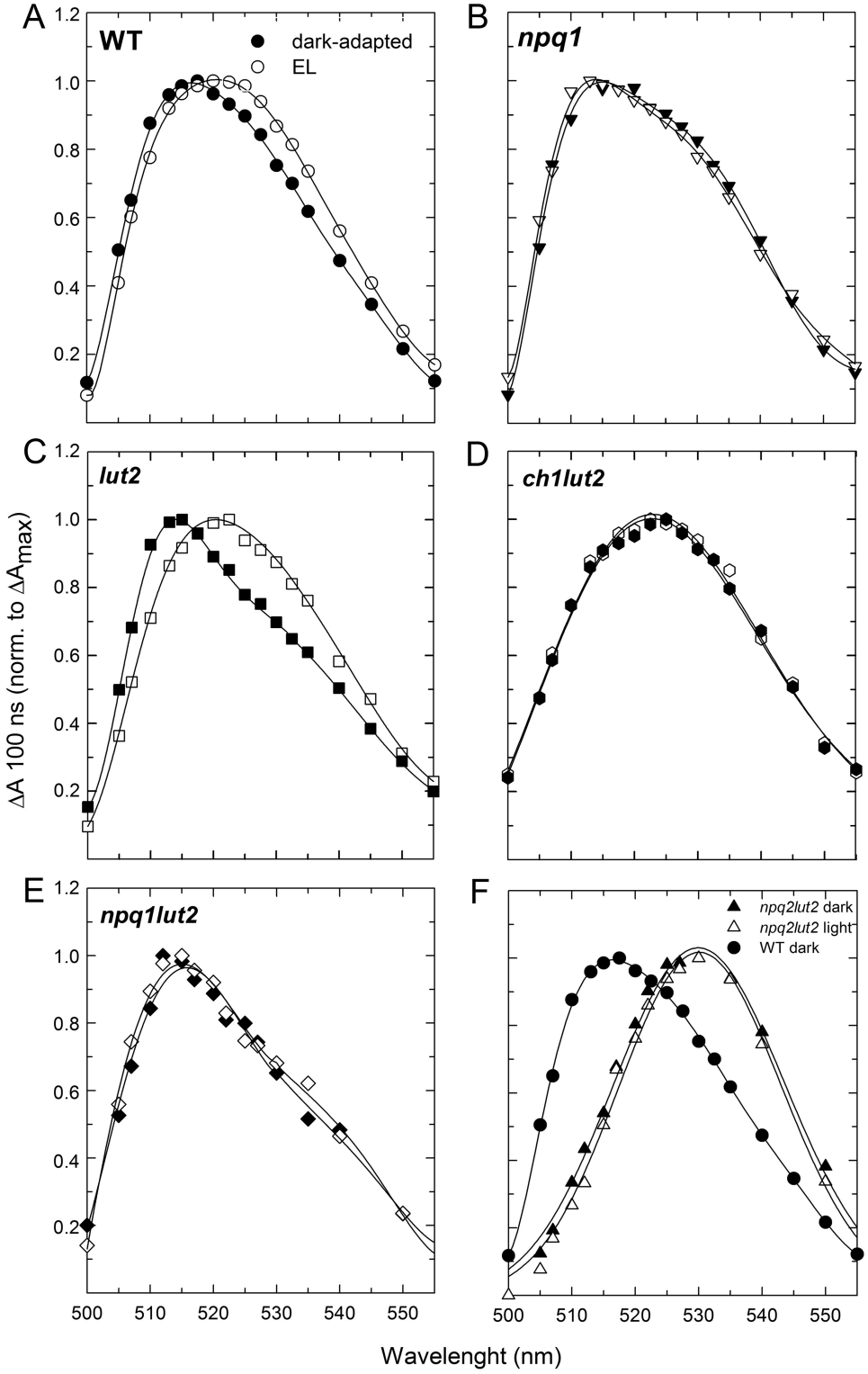

FIGURE 4. **Light-induced red shift of the carotenoid triplet transition on intact leaves.** Carotenoid triplet signal (difference between the spectra at 100 ns and 30 μs) was registered on *Arabidopsis* WT leaves either dark-adapted (*closed symbols*) or treated with EL (*open symbols*) upon vacuum infiltration with Norfluorazon to stabilize Zea content during measurements (see "Experimental Procedures" for details). Briefly, the same dark-adapted leaf, without being removed from the sample holder, was then illuminated with a continuous red light (630 nm $< \lambda <$ 700 nm, 1500 μmol of photons m^{-2} s^{-1}). After 15 min of exposure to the red light, the triplet signal was measured again. TmS spectra were recorded on leaves from WT (*A*), *npq1* (*B*), *lut2* (*C*), *ch1lut2* (*D*), and *npq1lut2* (*E*). In *panel F*, spectra of leaves from mutant *npq2lut2* (*triangles*), which constitutively accumulates Zea, are compared with the carotenoid triplet transition measured on dark-adapted WT leaves (*closed circles*).

than one solution, the fits given in Fig. 6 give a likely estimation of the total amount of ^{3}Car* formed upon excitation of Chls in the two samples. Both TmS spectra were described using single ^{3}Vio*, ^{3}Lutein* (^{3}Lut*), and ^{3}Zea* forms; the spectra of the CP26-Vio and CP26-Zzea complexes fit well by using similar spectral forms of ^{3}Vio* and ^{3}Lut*, whereas a

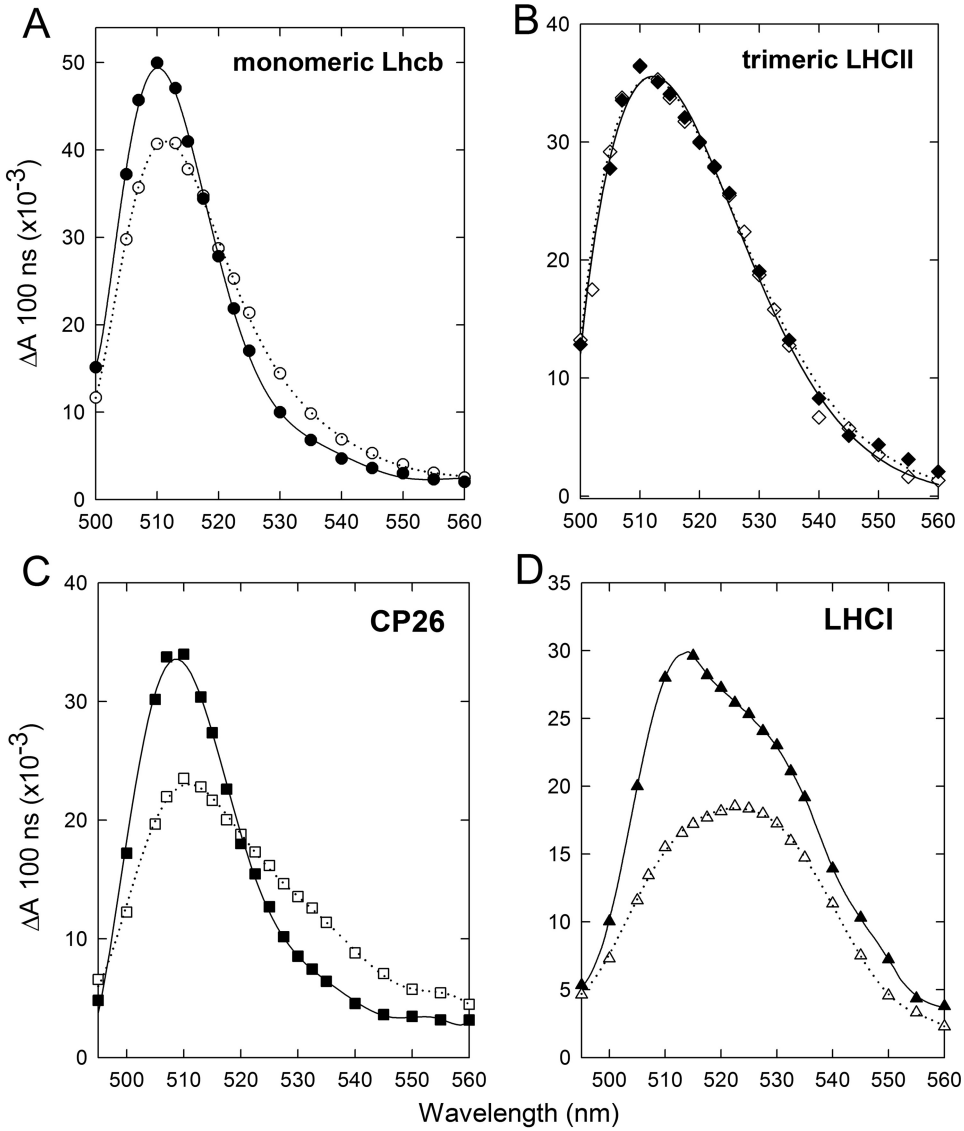

FIGURE 5. **Zea-induced red shift of the carotenoid triplet transition on isolated Lhc.** Spectral changes in the carotenoid triplet signal were detected in Lhc proteins isolated from *Arabidopsis* WT before and after EL exposure, leading to partial replacement of Vio by Zea in the protein complexes. Measurements were performed on either monomeric Lhcb (*A*), trimeric LHCII (*B*), the minor antenna CP26 (*C*), and the PSI-LHCI (*D*) proteins purified from dark-adapted (*closed symbols*) or EL-treated (*open symbols*) leaves.

^{3}Zea* form was necessary to fit the CP26-Zea TmS spectrum (Fig. 6, *A* and *B*).

The contributions of each xanthophyll to the total amount of ^{3}Car* formed were determined by using both the amplitudes in TmS spectra and ^{3}Car* extinction coefficients (ϵ_T) measured on isolated xanthophylls (Table 1) and are shown in Fig. 6*C*. In the CP26-Zea sample, the contributions of both ^{3}Vio* and ^{3}Lut* (which are reduced with respect to CP26-Vio sample) are compensated by formation of ^{3}Zea* (Fig. 6*C*).

To assess the kinetics of ^{3}Car* formation on purified CP26, time-resolved absorbance changes were recorded at two distinct wavelengths, corresponding to the maximum absorbance of ^{3}Vio* + ^{3}Lut* (510 nm) and ^{3}Zea* (530 nm). Similar half-times for both ^{3}Car* rise and decay (supplemental Fig. S5) were determined at both wavelengths, implying no differences in the ^{3}Chl* quenching capacity of CP26-bound Zea *versus* Vio.

In light of these findings, we attempted to verify the alternative hypothesis of direct modulation of ^{3}Chl* yield upon binding of Vio *versus* Zea independent from the quenching by xanthophylls. To this aim, we used FDMR. FDMR is a double resonance technique based on the principle that when a triplet steady state population is generated by illumination, application of a resonant electromagnetic field between a couple of spin sublevels of the triplet state induces a change in the steady state population of the triplet state itself due to anisotropy of the decay and population rates of the three spin sublevels. In FDMR experiments, the change induced in the triplet population is detected as a corresponding change in the emission of the system (60, 61). The activity of the carotenoids in quenching triplet states was investigated at low temperature (1.8 K), when the funneling of the excitation toward the low lying excited states of the Chl molecules is fast.

The low temperature emission spectrum of thylakoids from *Arabidopsis* WT showed the characteristic Chl *a* fluorescence bands peaking at 685–695 and 735 nm due to the different antenna pools belonging to PSII and PSI, in agreement with

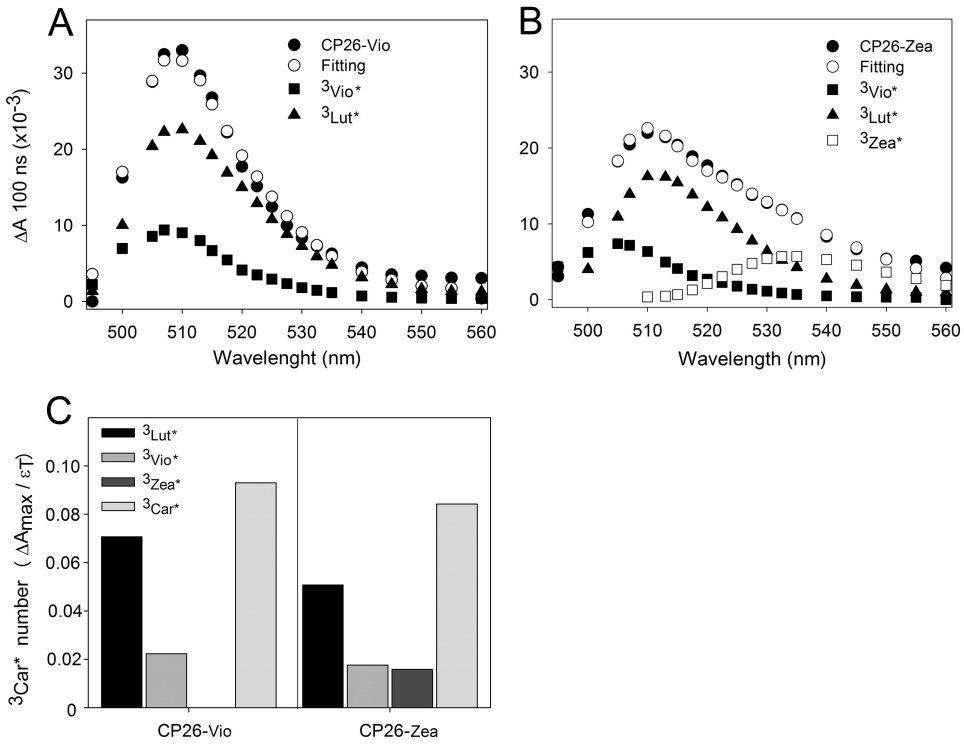

FIGURE 6. **Decomposition of CP26 TmS spectra.** Fitting of CP26 purified from leaves either dark-adapted (*A*) or treated with EL (*B*) was performed using absorption forms for xanthophyll triplets in protein environment. Components peaking at 507 and 510 nm were attributed to ^{3}Vio* and ^{3}Lut*, respectively, whereas the spectral form at 532 nm was attributed to ^{3}Zea*. In *panel C*, the amplitude of each spectral forms and the values of ϵ_T (Table 1) were used to calculate the number of triplet excited states formed upon excitation of Chl at 650 nm. The total carotenoid triplets (^{3}Car*) calculated from the spectral analysis were very similar in both samples.

literature data (data not shown). The FDMR signals, detected at 680–690 (PSII) and 720 nm (PSI), which represent transitions of ^{3}Chl* states, are shown in Fig. 7*A*. The three FDMR transitions with the polarization pattern usually found for ^{3}Car*, detected at 690 and 730 nm, are presented in Fig. 7*B* (44–46, 62). Two ^{3}Chl* components (visible in the 690 nm FDMR spectra), with $|D| - |E|/|D| + |E|$ transitions at about 725/945 and 742/965 MHz, have been previously assigned to the PSII outer antennae, whereas the 767/992-MHz component has been attributed to the core complex (45) (note that the signals have been reversed in sign compared with Ref. 48 for better representation). The ^{3}Car* states detected at 690 nm has been assigned to the PSII Lhcs (45). The negative signal at ~1000 MHz in the $|D| - |E|$ spectrum of ^{3}Car* in thylakoids (Fig. 7*B*) is the contribution of the ^{3}Chl* state from the PSII core complex (992 MHz component). The amplitude of this signal is enhanced due to the high frequency modulation (325 Hz) used for the ^{3}Car* measurement because of its fast decay (48). Other slower ^{3}Chl* components are not detected at this frequency (63).

The FDMR spectra of the thylakoids isolated from dark-adapted *npq1* leaves were identical to those of the sample from WT in the entire detection range explored (Fig. 7*C*). When measurements were performed on thylakoids isolated from WT EL-treated leaves (see supplemental Table S3 for pigment composition of thylakoids used), a decrease (−25%) in the intensity of the FDMR signals assigned to two ^{3}Chl* states belonging to PSII ($|D| - |E|$ transitions at 742 and 767 MHz) was observed. Also, a new component (719/992 MHz) appeared that can be assigned to the P_{680} recombination triplet state (64). Interestingly, in the thylakoids isolated from *npq1* EL-treated leaves, the intensity of the 742 MHz component did not undergo any decrease. A decreased amplitude was observed for the 767-MHz component, with a corresponding increase in the 720 MHz component (Fig. 7*C*). Except for the lack of the ^{3}P680* state formation, similar results were obtained on thylakoids isolated from dark-adapted WT and *npq1* leaves and de-epoxidated in the dark by incubating thylakoids at pH 5.2 (supplemental Fig. S6), implying that Zea itself, rather than the light treatment, is responsible for the spectral changes observed.

The FDMR signals of the ^{3}Car* states were sensitive to the treatments performed on the sample; the prolonged EL exposure induced a decrease of the intensity of the signals in WT thylakoids, whereas the effect was not evident in the *npq1* thylakoids (Fig. 7*D*). It should be noticed that carotenoids triplet states were observed in the presence of Zea, however, not with an increased yield. Lut and Zea contributions to the FDMR signal cannot be distinguished, as they have the same resonance frequencies as detected by comparing spectra from *npq2lut2* genotypes, containing Zea as the only carotenoid with the *npq2* containing Lute and Zea (not shown). Although FDMR cannot ascertain if Zea triplet states are or not populated at all, it is clear that the carotenoid triplet yield does not increase and does not correlate with the decrease of the ^{3}Chl* population in the presence of Zea. Once identified, the Zea-dependent effect on modulation of ^{3}Chl* populations in thylakoids was tracked to the individual pigment-protein components by performing the

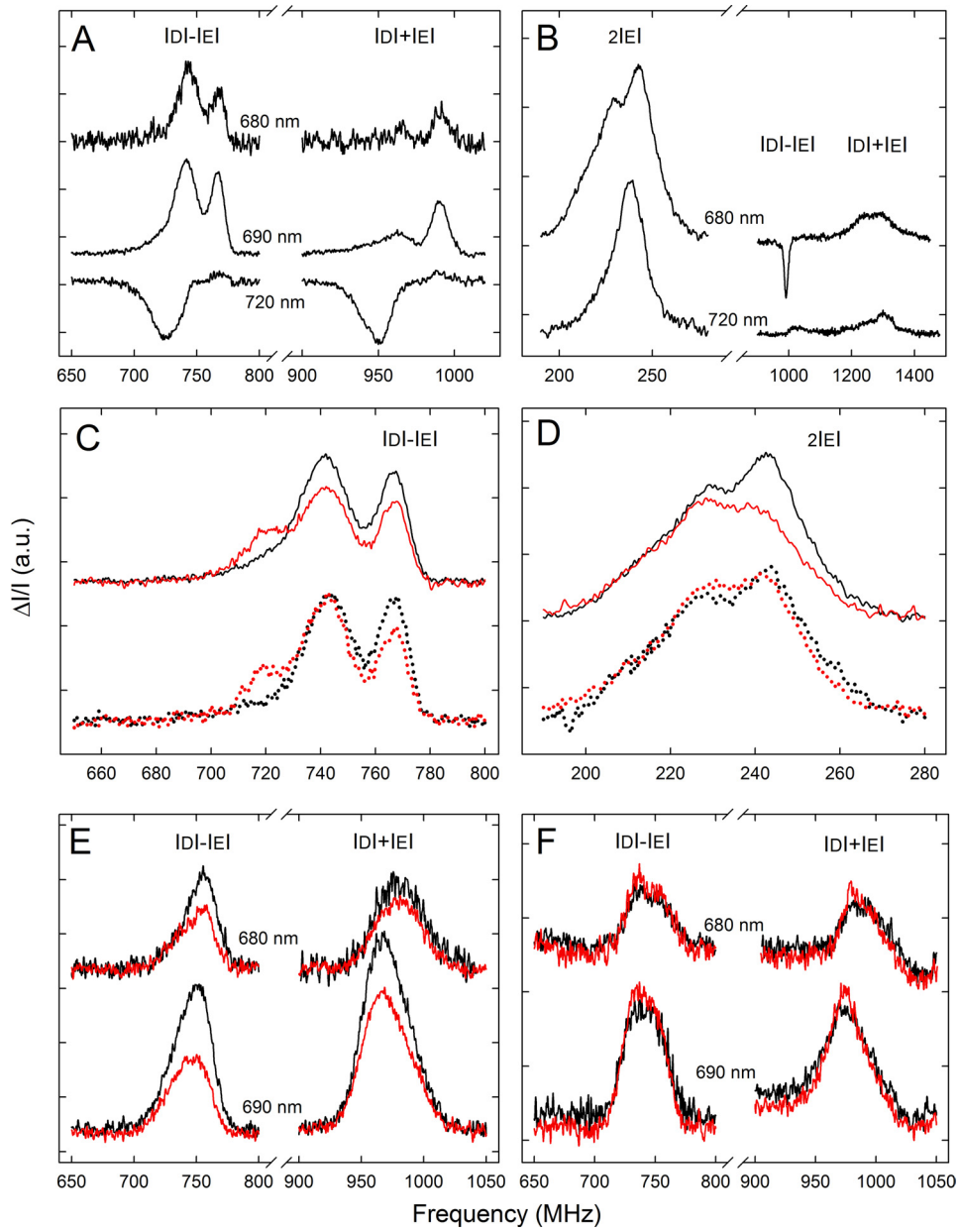

FIGURE 7. **Fluorescence detected magnetic resonance of the chlorophyll and carotenoid triplet states on thylakoids and isolated Lhc.** *A* and *B*, FDMR signals of the ^{3}Chl* states ($|D| - |E|$ and $|D| + |E|$ transitions) (*A*) and the ^{3}Car* states (*B*) observed in the WT thylakoid, dark-adapted sample, were detected at different wavelengths. *C*, $|D| - |E|$ transitions of the ^{3}Chl* states observed in the WT (*solid*) and *npq1* (*dotted*) thylakoids are shown. *Black*, dark-adapted; *red*, EL exposure. *a.u.*, absorbance units. *D*, shown are $2|E|$ transitions of the ^{3}Car* states, observed in the WT (*solid*) and in the *npq1* (*dotted*) thylakoids. *Black*, dark-adapted; *red*, EL exposure. *E*, FDMR signals of the ^{3}Chl* states of the minor antennae of WT detected at 680 and 690 nm are shown; dark-adapted samples are in *black*; samples isolated after EL irradiation are in *red*. *F*, FDMR signals of the ^{3}Chl* states of the trimeric LHCII of WT detected at 680 and 690 nm; dark-adapted samples are in *black*; samples isolated after EL irradiation are in *red*. Spectra have been vertically shifted for better comparison. Amplitude modulation frequency: 33 Hz (^{3}Chl* states) and 325 Hz, (^{3}Car* states), tc 600 ms, number of scans 20, mw power 500 milliwatt, temperature 1.8 K. *tc*, time constant; *mw*, microwaves.

same measurements on the different proteins isolated from WT leaves, either dark-adapted or treated with EL (Fig. 7*E*).

The ratio between the intensities of $|D| - |E|/|D| + |E|$ transitions of ^{3}Chl* are different in isolated Lhcs (Fig. 7*E*) with respect to thylakoids (Fig. 7*A*). Amplitudes of these transitions are sensitive to the environment of the triplet states; indeed ^{3}Chl* states show variable amplitudes in the two transitions due to changes in both populations and decay probabilities of the triplet sublevels. In thylakoids, the presence of interacting complexes creates a protein environment different than the detergent micelles of the isolated Lhcs. Moreover, FDMR spectra of thylakoids also contain the contribution from the PSII inner antenna subunits (767/992 MHz), absent in purified Lhcs.

Again, the Lhcbs affected by the light irradiation were the monomeric Lhcb4–6 proteins rather than the major LHCII complex. In Fig. 7*E*, the FDMR signals of ^{3}Chl* states detected at two different wavelengths show a decrease in intensity of 40% in the monomeric antenna fraction when binding Zea *versus* Vio. We did not observe any increase of the ^{3}Car* states correlated to the decrease of the ^{3}Chl* states. No change on the

triplet states FDMR signals was detected in the samples from *npq1,* and the FDMR spectra of isolated trimeric LHCII from WT and *npq1* were both insensitive to EL exposure of leaves previous to isolation (Fig. 7*F*). Establishing if the subset of chromophores-forming triplets is the same in both thylakoids and Lhcs is not straightforward. However, the effect of EL on the ^{3}Chl* yield is the same in both the minor Lhcbs and in thylakoids, suggesting these triplets have the same origin.

DISCUSSION

In this work we have scrutinized the mechanisms that contribute to the photoprotective effect of Zea, the xanthophyll specially synthesized in response to EL conditions. Previous work indicated that Zea synthesis has multiple effects. Earlier reports have emphasized the enhancing effect on qE, the PsbS-dependent thermal dissipation of ^{1}Chl* excited states (11, 14), and the uncoupler-resistant component called irreversible quenching or, more recently, qZ (51). A second photoprotective effect was reported to consist of a scavenging effect of lipid-free Zea for ROS released from Chl binding complexes (22, 29). A Zea-enhanced scavenging effect was also reported within Lhc proteins (30, 65). Although these functions contribute to the Zea photoprotective effect, genetic dissection showed that thermal dissipation of excess energy dissipation has a relatively small effect as assessed using the *npq4* mutant lacking qE (66) and likewise for the scavenging effect of lipid-free Zea with respect to the Lhc-bound fraction (Fig. 1). This implies that the Zea-dependent photoprotection effect is associated to the binding of Zea to Lhc proteins, where it has a strong effect in decreasing $^1O_2$ evolution during illumination. Here, we used high sensitivity laser spectroscopy to investigate changes in the optical properties of leaves associated with EL treatment. Illumination of *Arabidopsis* wild type plants induced a spectral red shift of the $T_2 \leftarrow T_1$ transition of ^{3}Car*. Using a range of *Arabidopsis* mutants, this spectroscopic feature was observed only in genotypes able to accumulate Zea, either upon EL exposure or constitutively (Fig. 5), irrespective of their the ability to perform qE (supplemental Fig. S4) and was coupled to a modulation of ^{3}Chl* yield, suggesting this mechanism is a component of photoprotection.

A Mechanism of Photoprotection Based on ^{3}Chl Down-regulation*—Because the TmS red shift involves the major ^{3}Car* transition, we first investigated if Zea had an enhanced ^{3}Chl* quenching capacity with respect to the pre-existing Viola, thus yielding a lower level of ^{3}Chl* formation. However, this was not confirmed by experimental evidences as (i) although not entirely resolved due to the 10 ns limitation in time resolution of our spectrophotometer, the kinetics of ^{3}Car* population was the same in Vio (510 nm) and Zea (530 nm) binding CP26 (supplemental Fig. 5), (ii) the relatively similar extinction coefficients of ^{3}Zea* and ^{3}Vio* (Fig. 6 and Table 1) imply that the decrease in the 510-nm band (^{3}Vio*) appears to be compensated by a similar increase of the 530-nm (^{3}Zea*) component in the spectra of Fig. 5*C* without a major difference in quenching efficiency between Zea and Vio, and (iii) a slight decrease in the ^{3}Car* level was detected by both laser spectroscopy (Fig. 6) and FDMR (Fig. 7*D*) in Zea *versus* Vio binding complexes. Rather, FDMR measurements showed that Zea binding to Lhc proteins induces a down-regulation of the ^{3}Chl* yield of the complexes (Fig. 7*E*) and whole thylakoids (Fig. 7*C*), likely through a mechanism different from the previously described triplet energy transfer to xanthophyll ligands (56, 67). The spectra are taken at 1.8 K; however, the samples adapted at RT were frozen by direct immersion on liquid helium into the cryostat, and therefore, the spectra are representative of the conformational distribution present at RT. It should be noted that the decrease in the concentration of ^{3}Chl* on both thylakoids and minor antennae cannot be ascribed to the residual quenching of ^{1}Chl* observed (68) upon EL treatment, as the procedure for thylakoid isolation is long enough to allow complete relaxation of NPQ induced by EL on leaves (19); the small quenching of ^{1}Chl* measured upon binding of Zea to minor antennae (about 10% than the corresponding sample from dark-adapted WT leaves, data not shown) cannot account for a 40% decrease in the concentration of ^{3}Chl* in these complexes (Fig. 7*E*). Moreover, FDMR signals are normalized to the amplitude of the steady state fluorescence. Thus, if the lower ^{3}Chl* yield was only due to the quenching of the corresponding singlet states, a decrease in the FDMR signal of the same level would be expected; instead, the decrease in the ^{3}Chl* yield in thylakoids upon EL treatment was ~25% (Fig. 7*C*) without a change in steady state fluorescence (not shown).

It is well known that CP26 and other Zea binding Lhc subunits undergo a conformational change upon exchange of Vio to Zea (51). We suggest that this conformational change, by affecting Chl-Chl and/or Chl-protein interactions, does modulate the triplet yield of the chlorophyll ligands and thus down-regulates the probability of reaction with O_2 and, subsequently, $^1O_2$ formation. Zea binding to Lhc proteins has at least two effects that may be correlated to each other or may not; that is, (*a*) quenching of ^{1}Chl* excited states and (*b*) decrease in ^{3}Chl* yield.

The relationship between the small change in fluorescence yield and the large change in triplet yield undergone by monomeric Lhc proteins upon binding of Zea is not clearly understood. An efficient thermal deactivation of ^{3}Chl* once they are formed appears unlikely because it requires intersystem crossing, making it a relatively slow process. A weak ^{1}Chl* quenching effect can be accounted for by an effect limited to a subset of chlorophylls in the pigment-protein complex. Such an effect could be produced by one of the following mechanisms; (i) the conformational change induced by Zea binding causes excitons in Chls bound to such a domain to be diverted from the sites where ^{3}Chl* are formed with higher yield (*i.e.* the red-most sites such as Chl A2, A4), possibly due to changes in the energy level of the former Chls (69), or (ii) alternatively, Chls generating triplet states with higher yield might become more readily quenched when still at their ^{1}Chl* state via thermal relaxation (70, 71). In such case, the singlet quenching would be limited to a subset of Chls of limited amplitude when refereed to the whole complex (52, 68, 72), whereas the effect on triplet state would be stronger.

Quenching of singlet states during short term light adaptation (qE) has been shown to be correlated to energy transfer from the Chl Q_y transition and the short-living ^{1}Car* state followed by thermal deactivation via the formation of a Chl^-/

Car^+ radical pair (18, 69). Such a mechanism could also favor $^3Chl^*$ to ^1Car energy transfer. However, the radical pair formation has been shown to require both the synthesis of Zea and the presence of a trans-membrane pH gradient, whereas its yield coefficient is far lower in isolated Lhc (18); this evidence is not consistent with the 40% reduction in $^3Chl^*$ yield detected in isolated pigment-protein complexes (Fig. 7).

Alternatively, the modulation of $^3Chl^*$ yield might be independent from the formation of radical pairs. Whatever the physical mechanism involved, the physiological effect is strong and produces effective photoprotection.

$^3Chl^*$ Down-regulation and PSII Supercomplex Organization—The search for fractions of thylakoid membranes exhibiting the red-shifted TmS spectrum and reduced FDMR $^3Chl^*$ signal yielded two major targets: monomeric Lhcb4–6 antenna subunits of PSII and LHCI. This is in agreement with previous work on Vio *versus* Zea exchange in different Lhc proteins during the operation of xanthophyll cycle (20, 53), as CP26 (Lhcb5), CP24 (Lhcb6), and Lhca4 were found to be the best "exchangers" among all Lhcs. Previous work with recombinant Lhc proteins (20) and *in vivo* (51) has shown that xanthophyll exchange is operated at the level of binding site L2 in both CP26 and LHCI. It would, therefore, appear that binding of Zea to Lhc proteins is sufficient for the modification of the triplet-state properties of the pigment-protein complexes, whereas the actual expression of this effect is controlled by the capacity for xanthophyll exchange in site L2 of the individual gene products. It should be noted that monomeric Lhcbs are located in between the PSII core complex and the outer antenna layer made by 2–4 copies of trimeric LHCII (75), each binding 42 Chls and 12 xanthophylls (26), implying most excitation energy collected by LHCII is funneled to the PSII reaction center through monomeric Lhcbs. Supplemental Fig. S2 clearly shows that, under EL conditions, Lhcb monomers get destroyed faster than LHCII unless they bind Zea that makes them more resistant to photodestruction.

A recent report demonstrated that, although xanthophyll ligands are very efficient in $^3Chl^*$ quenching, a limited fraction of $^3Chl^*$ cannot be quenched. In their original work, Mozzo *et al.* (56) measured a small amount of unquenched $^3Chl^*$ at physiological temperatures in LHCII. This is consistent with evidence that some Chls in purified LHCII, *e.g.* Chl 611 (26) were located too far apart from xanthophylls for efficient triplet transfer and can explain the bleaching of the complex when challenged with EL (76) (supplemental Fig. S2). In LHCII, ~5% of the triplets reside on Chls, corresponding to a 95% efficiency for Chl to Car triplet transfer (56); this value was lower for Lhcb5 and for Lhcb6 (52), reaching ~20% of unquenched $^3Chl^*$ in Vio binding complexes.

Results described here (Fig. 7) clearly show that even Chls in minor antennae, although active in singlet energy transfer (as assessed by fluorescence emission measurements), are not equally active in transferring triplets. It is well known that triplet transfer requires shorter distances between the chromophores than singlet transfer. The absence of a triplet transfer enhancement upon Zea synthesis on one hand and regulation of $^3Chl^*$ on the other, however, suggests that the binding of Zea in site L2 has an effect on the structure of the complex; it might result in an altered organization of protein domains to modulate the triplet yield of some chlorophylls rather than in a conformational change that reduces the proximity between unprotected chlorophylls and xanthophylls.

Why is Zea only present during stress conditions when it is effective in photoprotection? At least one reason, if not the only reason, is that massive binding of Zea to Lhc (such as in *npq2* mutant of *Arabidopsis*) is well known to strongly decrease the excited singlet state lifetime (77) of the plants. Therefore, plants that constitutively accumulate Zea can utilize less photons for charge separation, which decreases the growth rate in limiting light (51). We conclude that monomeric Lhcbs in WT PSII are present in two states, dark-adapted and EL, binding Vio and Zea, respectively, in their L2 sites. The dark-adapted state ensures a longer fluorescence lifetime and relatively high $^3Chl^*$ yield, which is not a problem due to efficient photochemical quenching in low light conditions. The EL state has a lower $^3Chl^*$ level and a shorter $^1Chl^*$ lifetime (68) than the dark-adapted state, which is well suited for photoprotection under these conditions. Besides Lhcbs, Zea also binds to Lhca polypeptides, which is so far unexplained under the widespread understanding that the major Zea function is to enhance qE due to the low level of excited states (short fluorescence lifetime) of PSI. Nevertheless, Lhca subunits host the red-most absorption forms that make a low energy trap for excitation energy before photochemical quenching by P700 (78). Because of the $^3Chl^*$ down-regulating effect of Zea, its binding to Lhcas may be understood as a photoprotection mechanism for highly localized excitons in Lhca3 and Lhca4, the red-most subunits in the PSI-LHCI supercomplex (79).

We have shown that Zea accumulation in chloroplasts under EL produced a red shift of the major carotenoid transition in the TmS spectra. These changes were measured on intact leaves and correlate with the amount of Zea accumulated in specific Lhc subunits located in between the major LHCII antenna complex and the reaction center in PSII supercomplexes and in LHCI. The resistance/sensitivity of these proteins to EL conditions indicated that the red shift is correlated with the dominant component of photoprotection, in absence of which monomeric Lhcbs are preferentially destroyed. The protection effect appears to consist with a direct down-regulation of $^3Chl^*$ without a corresponding triplet quenching enhancement by nearby xanthophylls. High resolution crystallography of Zea binding complexes will further assist with elucidating this new mechanism of photoprotection. After this manuscript was finished, the report by Carbonera *et al.* (73) was published, showing that $^3Chl^*$ concentration is strongly reduced upon high light treatment. Although this result is consistent with the present report, it refers to a component of photoprotection distinct from that discuss here. In fact, in Ref. 73 the protective effect was abolished by the *lhcsr1 lhcsr2 psbS* mutation abolishing qE. On the contrary, the zeaxanthin-dependent photoprotection component here described is fully active in the *npq4* mutant lacking PsbS (supplemental Fig. S4).

REFERENCES

1. Green, M. J., and Hill, H. A. (1984) Chemistry of dioxygen. *Methods Enzymol.* **105,** 3–22

2. Moan, J., and Berg, K. (1991) The photodegradation of porphyrins in cells can be used to estimate the lifetime of singlet oxygen. *Photochem. Photobiol.* **53,** 549–553
3. Girotti, A. W., and Kriska, T. (2004) Role of lipid hydroperoxides in photooxidative stress signaling. *Antioxid. Redox Signal.* **6,** 301–310
4. Martinez, G. R., Loureiro, A. P., Marques, S. A., Miyamoto, S., Yamaguchi, L. F., Onuki, J., Almeida, E. A., Garcia, C. C., Barbosa, L. F., Medeiros, M. H., and Di Mascio, P. (2003) Oxidative and alkylating damage in DNA. *Mutat. Res.* **544,** 115–127
5. Davies, M. J. (2004) Reactive species formed on proteins exposed to singlet oxygen. *Photochem. Photobiol. Sci.* **3,** 17–25
6. Harvaux, M., and Kloppstech, K. (2001) The protective functions of carotenoid and flavonoid pigments against excess visible radiations at chilling temperature investigated in *Arabidopsis npq* and *tt* mutants. *Planta* **213,** 953–966
7. Kok, B. (1956) On the inhibition of photosynthesis by intense light. *Biochim. Biophys. Acta* **21,** 234–244
8. Aro, E. M., Virgin, I., and Andersson, B. (1993) Photoinhibition of Photosystem-2. Inactivation, protein damage, and turnover. *Biochim. Biophys. Acta* **1143,** 113–134
9. Long, S. P., Humphries, S., and Falkowski, P. G. (1994) Photoinhibition of photosynthesis in nature. *Annu. Rev. Plant Physiol. Plant Mol. Biol.* **45,** 633–662
10. Frank, H. A., and Cogdell, R. J. (1996) Carotenoids in photosynthesis. *Photochem. Photobiol.* **63,** 257–264
11. Niyogi, K. K., Grossman, A. R., and Björkman, O. (1998) *Arabidopsis* mutants define a central role for the xanthophyll cycle in the regulation of photosynthetic energy conversion. *Plant Cell* **10,** 1121–1134
12. Mathis, P., Butler, W. L., and Satoh, K. (1979) Carotenoid triplet state and chlorophyll fluorescence quenching in chloroplasts and subchloroplasts particles. *Photochem. Photobiol.* **30,** 603–614
13. El-Agamey, A., Lowe, G. M., McGarvey, D. J., Mortensen, A., Phillip, D. M., Truscott, T. G., and Young, A. J. (2004) Carotenoid radical chemistry and antioxidant/pro-oxidant properties. *Arch. Biochem. Biophys.* **430,** 37–48
14. Demmig-Adams, B., Winter, K., Kruger, A., and Czygan, F.-C. (1989) in *Photosynthesis. Plant Biology* (Briggs, W. R., ed) Vol. 8, Alan R. Liss, New York
15. Bugos, R. C., and Yamamoto, H. Y. (1996) Molecular cloning of violaxanthin de-epoxidase from romaine lettuce and expression in *Escherichia coli*. *Proc. Natl. Acad. Sci. U.S.A.* **93,** 6320–6325
16. Arnoux, P., Morosinotto, T., Saga, G., Bassi, R., and Pignol, D. (2009) A structural basis for the pH-dependent xanthophyll cycle in *Arabidopsis thaliana*. *Plant Cell* **21,** 2036–2044
17. Niyogi, K. K., Bjorkman, O., and Grossman, A. R. (1997) Chlamydomonas xanthophyll cycle mutants identified by video imaging of chlorophyll fluorescence quenching. *Plant Cell* **9,** 1369–1380
18. Holt, N. E., Zigmantas, D., Valkunas, L., Li, X. P., Niyogi, K. K., and Fleming, G. R. (2005) Carotenoid cation formation and the regulation of photosynthetic light harvesting. *Science* **307,** 433–436
19. Nilkens, M., Kress, E., Lambrev, P., Miloslavina, Y., Müller, M., Holzwarth, A. R., and Jahns, P. (2010) Identification of a slowly inducible zeaxanthin-dependent component of non-photochemical quenching of chlorophyll fluorescence generated under steady-state conditions in *Arabidopsis*. *Biochim. Biophys. Acta* **1797,** 466–475
20. Morosinotto, T., Baronio, R., and Bassi, R. (2002) Dynamics of chromophore binding to Lhc proteins *in vivo* and *in vitro* during operation of the xanthophyll cycle. *J. Biol. Chem.* **277,** 36913–36920
21. Walters, R. G., and Horton, P. (1991) Resolution of components of non-photochemical chlorophyll fluorescence quenching in barley leaves. *Photosynth. Res.* **27,** 121–133
22. Havaux, M., and Niyogi, K. K. (1999) The violaxanthin cycle protects plants from photooxidative damage by more than one mechanism. *Proc. Natl. Acad. Sci. U.S.A.* **96,** 8762–8767
23. Külheim, C., Agren, J., and Jansson, S. (2002) Rapid regulation of light harvesting and plant fitness in the field. *Science* **297,** 91–93
24. Havaux, M., Dall'Osto, L., Cuiné, S., Giuliano, G., and Bassi, R. (2004) The effect of zeaxanthin as the only xanthophyll on the structure and function of the photosynthetic apparatus in *Arabidopsis thaliana*. *J. Biol. Chem.* **279,** 13878–13888
25. Caffarri, S., Croce, R., Breton, J., and Bassi, R. (2001) The major antenna complex of photosystem II has a xanthophyll binding site not involved in light harvesting. *J. Biol. Chem.* **276,** 35924–35933
26. Liu, Z., Yan, H., Wang, K., Kuang, T., Zhang, J., Gui, L., An, X., and Chang, W. (2004) Crystal structure of spinach major light-harvesting complex at 2.72 Å resolution. *Nature* **428,** 287–292
27. Jahns, P., Latowski, D., and Strzalka, K. (2009) Mechanism and regulation of the violaxanthin cycle. The role of antenna proteins and membrane lipids. *Biochim. Biophys. Acta* **1787,** 3–14
28. Morosinotto, T., Caffarri, S., Dall'Osto, L., and Bassi, R. (2003) Mechanistic aspects of the xanthophyll dynamics in higher plant thylakoids. *Physiol. Plant.* **119,** 347–354
29. Havaux, M., Dall'osto, L., and Bassi, R. (2007) Zeaxanthin has enhanced antioxidant capacity with respect to all other xanthophylls in *Arabidopsis* leaves and functions independent of binding to PSII antennae. *Plant Physiol.* **145,** 1506–1520
30. Dall'Osto, L., Cazzaniga, S., Havaux, M., and Bassi, R. (2010) Enhanced photoprotection by protein-bound *versus* free xanthophyll pools. A comparative analysis of chlorophyll *b* and xanthophyll biosynthesis mutants. *Mol. Plant* **3,** 576–593
31. Hartel, H., Lokstein, H., Grimm, B., and Rank, B. (1996) Kinetic studies on the xanthophyll cycle in barley leaves (influence of antenna size and relations to Nonphotochemical chlorophyll fluorescence quenching). *Plant Physiol.* **110,** 471–482
32. Havaux, M., Bonfils, J. P., Lütz, C., and Niyogi, K. K. (2000) Photodamage of the photosynthetic apparatus and its dependence on the leaf developmental stage in the *npq1 Arabidopsis* mutant deficient in the xanthophyll cycle enzyme violaxanthin de-epoxidase. *Plant Physiol.* **124,** 273–284
33. Casazza, A. P., Tarantino, D., and Soave, C. (2001) Preparation and functional characterization of thylakoids from *Arabidopsis thaliana*. *Photosynth. Res.* **68,** 175–180
34. Morosinotto, T., Bassi, R., Frigerio, S., Finazzi, G., Morris, E., and Barber, J. (2006) Biochemical and structural analyses of a higher plant photosystem II supercomplex of a photosystem I-less mutant of barley. Consequences of a chronic over-reduction of the plastoquinone pool. *FEBS J.* **273,** 4616–4630
35. Dainese, P., Hoyer-hansen, G., and Bassi, R. (1990) The resolution of chlorophyll *a*/*b*-binding proteins by a preparative method based on flat bed isoelectric focusing. *Photochem. Photobiol.* **51,** 693–703
36. Croce, R., and Bassi, R. (1998) in *Photosynthesis: Mechanisms and Effects* (Garab, G., ed) Vol. I, pp 421–424, Kluwer Academic Press, Dordrecht, The Netherlands
37. Gilmore, A. M., and Yamamoto, H. Y. (1991) Zeaxanthin formation and energy-dependent fluorescence quenching in pea chloroplasts under artificially mediated linear and cyclic electron transport. *Plant Physiol.* **96,** 635–643
38. León, R., Vila, M., Hernánz, D., and Vílchez, C. (2005) Production of phytoene by herbicide-treated microalgae *Dunaliella bardawil* in two-phase systems. *Biotechnol. Bioeng.* **92,** 695–701
39. Towbin, H., Staehelin, T., and Gordon, J. (1979) Electrophoretic transfer of proteins from polyacrylamide gels to nitrocellulose sheets. Procedure and some applications. *Proc. Natl. Acad. Sci. U.S.A.* **76,** 4350–4354
40. Beal, D., Rappaport, F., and Joliot, P. (1999) A new high-sensitive 10-ns time-resolution spectrophotometric technique adapted to *in vivo* analysis of the photosynthetic apparatus. *Rev. Sci. Instrum.* **70,** 202–207
41. Flors, C., Fryer, M. J., Waring, J., Reeder, B., Bechtold, U., Mullineaux, P. M., Nonell, S., Wilson, M. T., and Baker, N. R. (2006) Imaging the production of singlet oxygen *in vivo* using a new fluorescent sensor, singlet oxygen sensor green. *J. Exp. Bot.* **57,** 1725–1734
42. Driever, S. M., Fryer, M. J., Mullineaux, P. M., and Baker, N. R. (2009) Imaging of reactive oxygen species *in vivo*. *Methods Mol. Biol.* **479,** 109–116
43. de Bianchi, S., Betterle, N., Kouril, R., Cazzaniga, S., Boekema, E., Bassi, R., and Dall'Osto, L. (2011) *Arabidopsis* mutants deleted in the light-harvesting protein Lhcb4 have a disrupted Photosystem II macrostructure and are defective in photoprotection. *Plant Cell* **23,** 2659–2679

44. Carbonera, D., Giacometti, G., and Agostini, G. (1992) FDMR of carotenoid and chlorophyll triplets in light-harvesting complex LHCII of spinach. *Appl. Magn. Reson.* **3,** 361–368
45. Santabarbara, S., Bordignon, E., Jennings, R. C., and Carbonera, D. (2002) Chlorophyll triplet states associated with photosystem II of thylakoids. *Biochemistry* **41,** 8184–8194
46. Santabarbara, S., Agostini, G., Heathcote, P., and Carbonera, D. (2005) A fluorescence detected magnetic resonance investigation of the carotenoid triplet states associated with photosystem II of isolated spinach thylakoid membranes. *Photosynth. Res.* **86,** 283–296
47. Tanaka, A., Ito, H., Tanaka, R., Tanaka, N. K., Yoshida, K., and Okada, K. (1998) Chlorophyll a oxygenase (CAO) is involved in chlorophyll *b* formation from chlorophyll *a*. *Proc. Natl. Acad. Sci. U.S.A.* **95,** 12719–12723
48. Plumley, F. G., and Schmidt, G. W. (1987) Reconstitution of chloroform *a*/*b* light-harvesting complexes. Xanthophyll-dependent assembly and energy transfer. *Proc. Natl. Acad. Sci. U.S.A.* **84,** 146–150
49. Kim, E. H., Li, X. P., Razeghifard, R., Anderson, J. M., Niyogi, K. K., Pogson, B. J., and Chow, W. S. (2009) The multiple roles of light-harvesting chlorophyll *a*/*b*-protein complexes define structure and optimize function of *Arabidopsis* chloroplasts. A study using two chlorophyll *b*-less mutants. *Biochim. Biophys. Acta* **1787,** 973–984
50. Triantaphylidès, C., Krischke, M., Hoeberichts, F. A., Ksas, B., Gresser, G., Havaux, M., Van Breusegem, F., and Mueller, M. J. (2008) Singlet oxygen is the major reactive oxygen species involved in photooxidative damage to plants. *Plant Physiol.* **148,** 960–968
51. Dall'Osto, L., Caffarri, S., and Bassi, R. (2005) A mechanism of nonphotochemical energy dissipation, independent from Psbs, revealed by a conformational change in the antenna protein CP26. *Plant Cell* **17,** 1217–1232
52. Betterle, N., Ballottari, M., Hienerwadel, R., Dall'Osto, L., and Bassi, R. (2010) Dynamics of zeaxanthin binding to the photosystem II monomeric antenna protein Lhcb6 (CP24) and modulation of its photoprotection properties. *Arch. Biochem. Biophys.* **504,** 67–77
53. Wehner, A., Storf, S., Jahns, P., and Schmid, V. H. (2004) De-epoxidation of violaxanthin in light-harvesting complex I proteins. *J. Biol. Chem.* **279,** 26823–26829
54. Yakushevska, A. E., Jensen, P. E., Keegstra, W., van Roon, H., Scheller, H. V., Boekema, E. J., and Dekker, J. P. (2001) Supermolecular organization of photosystem II and its associated light-harvesting antenna in *Arabidopsis thaliana*. *Eur. J. Biochem.* **268,** 6020–6028
55. Dall'Osto, L., Lico, C., Alric, J., Giuliano, G., Havaux, M., and Bassi, R. (2006) Lutein is needed for efficient chlorophyll triplet quenching in the major LHCII antenna complex of higher plants and effective photoprotection *in vivo* under strong light. *BMC Plant Biology* **6,** 32
56. Mozzo, M., Dall'Osto, L., Hienerwadel, R., Bassi, R., and Croce, R. (2008) Photoprotection in the antenna complexes of photosystem II. Role of individual xanthophylls in chlorophyll triplet quenching. *J. Biol. Chem.* **283,** 6184–6192
57. Witt, H. T. (1979) Energy conversion in the functional membrane of photosynthesis. Analysis by light pulse and electric pulse methods. The central role of the electric field. *Biochim. Biophys. Acta* **505,** 355–427
58. Hiyama, T., and Ke, B. (1972) Difference spectra and extinction coefficients of P700*. *Biochim. Biophys. Acta* **267,** 160–171
59. Nielsen, B. R., Jorgensen, K., and Skibsted, L. H. (1998) Triplet-triplet extinction coefficients, rate constants of triplet decay, and rate constants of anthracene triplet sensitization by laser flash photolysis of astaxanthin, β-carotene, canthaxanthin, and zeaxanthin in deaerated toluene at 298 K. *J. Photochem. Photobiol. A Chem.* **112,** 127–133
60. Clarke, R. H. (1982) *Triplet State ODMR Spectroscopy. Techniques and Applications to Biophysical Systems* (Clarke, R. H., ed) Wiley, New York
61. Hoff, A. J. (1989) *Optically Detected Magnetic Resonance* (*ODMR*) *of triplet states in vivo* (Staehlin, L. A., ed) Elsevier, Amsterdam
62. Salvadori, E., Di Valentin, M., Kay, C. W., Pedone, A., Barone, V., and Carbonera, D. (2012) The electronic structure of the lutein triplet state in plant light-harvesting complex II. *Phys. Chem. Chem. Phys.* **14,** 12238–12251
63. Santabarbara, S., Jennings, R. C., and Carbonera, D. (2003) Analysis of photosystem II triplet states in thylakoids by fluorescence detected magnetic resonance in relation to the redox state of the primary quinone acceptor Q_A. *Chem. Phys.* **294,** 257–266
64. Carbonera, D., Giacometti, G., and Agostini, G. (1994) A well resolved ODMR triplet minus singlet spectrum of P680 from PSII particles. *FEBS Lett.* **343,** 200–204
65. Johnson, M. P., Havaux, M., Triantaphylidès, C., Ksas, B., Pascal, A. A., Robert, B., Davison, P. A., Ruban, A. V., and Horton, P. (2007) Elevated zeaxanthin bound to oligomeric LHCII enhances the resistance of *Arabidopsis* to photooxidative stress by a lipid-protective, antioxidant mechanism. *J. Biol. Chem.* **282,** 22605–22618
66. Li, X. P., Muller-Moule, P., Gilmore, A. M., and Niyogi, K. K. (2002) PsbS-dependent enhancement of feedback de-excitation protects photosystem II from photoinhibition. *Proc. Natl. Acad. Sci. U.S.A.* **99,** 15222–15227
67. Peterman, E. J., Dukker, F. M., van Grondelle, R., and van Amerongen, H. (1995) Chlorophyll *a* and carotenoid triplet states in light-harvesting complex II of higher plants. *Biophys. J.* **69,** 2670–2678
68. Moya, I., Silvestri, M., Vallon, O., Cinque, G., and Bassi, R. (2001) Time-resolved fluorescence analysis of the Photosystem II antenna proteins in detergent micelles and liposomes. *Biochemistry* **40,** 12552–12561
69. Ahn, T. K., Avenson, T. J., Ballottari, M., Cheng, Y. C., Niyogi, K. K., Bassi, R., and Fleming, G. R. (2008) Architecture of a charge-transfer state regulating light harvesting in a plant antenna protein. *Science* **320,** 794–797
70. Liao, P. N., Holleboom, C. P., Wilk, L., Kühlbrandt, W., and Walla, P. J. (2010) Correlation of Car S1 → Chl with Chl → Car S1 energy transfer supports the excitonic model in quenched light harvesting complex II. *J. Phys. Chem. B* **114,** 15650–15655
71. Liao, P. N., Pillai, S., Gust, D., Moore, T. A., Moore, A. L., and Walla, P. J. (2011) Two-photon study on the electronic interactions between the first excited singlet states in carotenoid-tetrapyrrole dyads. *J. Phys. Chem. A* **115,** 4082–4091
72. Wentworth, M., Ruban, A. V., and Horton, P. (2000) Chlorophyll fluorescence quenching in isolated light harvesting complexes induced by zeaxanthin. *FEBS Lett.* **471,** 71–74
73. Carbonera, D., Gerotto, C., Posocco, B., Giacometti, G. M., and Morosinotto, T. (2012) NPQ activation reduces chlorophyll triplet state formation in the moss *Physcomitrella patens*. *Biochim. Biophys. Acta* **1817,** 1608–1615
74. Deleted in proof
75. Caffarri, S., Kouril, R., Kereïche, S., Boekema, E. J., and Croce, R. (2009) Functional architecture of higher plant photosystem II supercomplexes. *EMBO J.* **28,** 3052–3063
76. Formaggio, E., Cinque, G., and Bassi, R. (2001) Functional architecture of the major light-harvesting complex from higher plants. *J. Mol. Biol.* **314,** 1157–1166
77. Gilmore, A. M., Shinkarev, V. P., Hazlett, T. L., and Govindjee (1998) Quantitative analysis of the effects of intrathylakoid pH and xanthophyll cycle pigments on chlorophyll a fluorescence lifetime distributions and intensity in thylakoids. *Biochemistry* **37,** 13582–13593
78. Croce, R., Dorra, D., Holzwarth, A. R., and Jennings, R. C. (2000) Fluorescence decay and spectral evolution in intact photosystem I of higher plants. *Biochemistry* **39,** 6341–6348
79. Croce, R., Morosinotto, T., Castelletti, S., Breton, J., and Bassi, R. (2002) The Lhca antenna complexes of higher plants photosystem I. *Biochim. Biophys. Acta* **1556,** 29–40
80. Britton, G., Liaaen-Jensen, S., and Pfander, H. (eds) (2004) *Carotenoids Vol. 1B: Spectroscopy*, pp. 57–61, Birkhauser Verlag, Basel, Switzerland